Mean-field analysis of pairing in asymmetric Fermi systems at finite temperature

Rishi Sharma* and Sanjay Reddy†
Theoretical Division, Los Alamos National Laboratory, MS-B283, Los Alamos, New Mexico 87545, USA
(Received 19 June 2008; revised manuscript received 20 August 2008; published 16 December 2008)

We study the phase diagram of a two component Fermi system with a weak attractive interaction. Our analysis includes the leading order Hartree energy shifts and pairing correlations at finite temperature and chemical potential difference between the two fermion species. We show that in an asymmetric system, the Hartree shift to the single particle energies is important for the phase competition between normal and superfluid phase and can change the phase transition curve qualitatively. At large chemical potential asymmetry we find that a somewhat fragile superfluid state can be favored due to finite-temperature effects. We also investigate the transition between the normal phase and an inhomogeneous superfluid phase to study how gradient instabilities evolve with temperature and asymmetry. Finally, we adopt our analysis to study the density profiles of similar asymmetric Fermi systems that are being observed in cold-atom experiments.

DOI: 10.1103/PhysRevA.78.063609 PACS number(s): 03.75.Ss, 74.25.Dw, 74.20.Fg

I. INTRODUCTION

The superfluid nature of the ground state of symmetric two-component Fermi systems, where pairing occurs between equal densities of the two species, has been well established, both on theoretical and experimental grounds, since the pioneering work of Bardeen, Cooper, and Schrieffer (BCS) 50 years ago [1]. However, the phase structure of asymmetric Fermi systems still remains unclear. In particular, theoretical work suggests that several competing superfluid phases may be possible. These include (i) the Ferrel, Fulde, Larkin, Ovchinnikov (FFLO) phase, which is an inhomogeneous superfluid phase with a spatially varying superfluid order parameter [2,3]; and (ii) phases with broken rotational symmetry where pairing is facilitated by a deformation of the Fermi surface [4,5]. Quantum Monte Carlo (QMC) calculations have been used to calculate the thermodynamic properties of a symmetric system at zero temperature [6] for arbitrary interaction strength. The authors of [7] used these results to deduce the presence of a splitting point at nonzero chemical potential asymmetry in the Bose-Einstein condensate (BEC) regime of the phase diagram, where the interaction is strong enough to support a two-body bound state in vacuum. At this splitting point, a gapped superfluid phase, a gapless superfluid phase, and an inhomogeneous superfluid phase coexist. This implies that in the BCS regime where the interaction does not support a bound state, a finite chemical potential difference would induce a quantum phase transition from the gapped superfluid state to an inhomogeneous phase prior to inducing a transition to the normal phase. The special point between the BCS and BEC regimes which is characterized by an infinite s-wave scattering length and is often called the unitary regime, is expected to exhibit similar qualitative behavior.

To investigate the possible existence of these phases, cold-atom experiments are now exploring the thermodynamic and linear response properties of asymmetric Fermi systems with attractive interactions [8–12]. These experiments which trap and cool two hyperfine states of ^{6}Li atoms, have unprecedented control over the sample. They can (i) magnetically tune the interaction strength between the two hyperfine states through Feshbach resonances; (ii) control the population asymmetry by loading different numbers of atoms; and (iii) vary the temperature. In the strongly interacting regime, where the two-body scattering length is large, these experiments have already observed how the superfluid properties change with number asymmetry and temperature. Experimental measurements of the density profiles and the response to radio frequency probes seem to indicate that these phases are not realized in cold-atom traps. Instead one finds strong indications of a first-order phase transition between a superfluid state with zero number asymmetry and a normal state with a large asymmetry [8,9].

The absence of intervening non-BCS superfluid phases in cold-atom experiments is intriguing. These phases may still exist at very low temperature and in the weak coupling regime. To address if these phases can be realized in experiments in the future, we investigate the phase structure of Fermi systems at finite temperature, T, and chemical potential asymmetry, $\delta\mu$, and establish the parameter region where interesting new phases of superfluidity can be realized.

The finite-temperature phase diagram of polarized cold-atomic gases has been studied previously [13–23]. We summarize the main results of these studies in the weak coupling (BCS) regime using a schematic phase diagram (Fig. 1). A key feature of the phase diagram in the $(\delta\mu, T)$ plane is the tricritical point (TCP), where the normal, the homogeneous superfluid, and the FFLO phase can coexist. This is the point where the putative first-order line separating the FFLO and the normal phase (FN_1) meets the second-order line between the normal and the homogeneous superfluid phase (SN_2). The authors of [13] found that this point coincides with (or at least lies very close to [14,15]) the point where a second-order line marking the instability of the normal phase towards the growth of inhomogeneous fluctuations, FN_2, meets SN_2, and we have drawn the figure reflecting this observation. At the curve marked SN_1, if we do not consider the FFLO phase, there would be a first-order phase transition

*rishi@lanl.gov
†reddy@lanl.gov

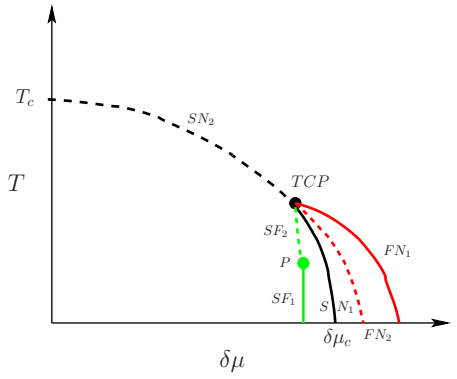

FIG. 1. (Color online) We show a schematic phase diagram in $\delta\mu, T$ space featuring the normal, homogeneous superfluid, and the FFLO phase. The curves are labeled by the phases they separate, S standing for homogeneous superfluid, F for FFLO, and N for normal. The subscript represents the order of the phase transition. TCP is the tricritical point. T_c refers to the critical temperature at $\delta\mu=0$, where there is a second-order transition from S to N. $\delta\mu_c$ is the Clogston point where there is a first-order transition from S to N at $T=0$.

between the normal and the superfluid phase. In reality though, this lies in the region where the true ground state is expected to be a FFLO phase, bounded by the homogeneous superfluid-FFLO boundary on the left (SF_1 and SF_2) and FN_1 on the right. We have left open the possibility that the homogeneous superfluid-FFLO boundary is first order at low temperatures (SF_1) and becomes second order (SF_2) at temperatures above those corresponding to some point P. It is possible that P coincides with the TCP, but we shall see below that when we include Hartree corrections, we find that there is a region in the homogeneous superfluid phase that is unstable to the growth of space-dependent fluctuations of the phase of the condensate (also known as the current instability). At the boundary of this unstable region, the transition from the FFLO to the homogeneous paired phase is second order, meaning that it is possible that P does not coincide with the TCP. From the topology of the diagram one can see that SF_2 must necessarily meet SN_2 at the TCP.

In our work, we look at how Hartree corrections affect the shape and the position of the curve labeled SN_1. We find that including the Hartree corrections shift the curve to larger values of $\delta\mu$ for a given interparticle coupling, and in addition changes its shape qualitatively. We also consider small, space-dependent fluctuations about the homogeneous superfluid phase and the normal phase, which will allow us to mark out the regions where these homogeneous phases become unstable to the formation of the FFLO phase. This analysis will not be able to find the location of the first-order curves separating these phases and the FFLO phase. For that one needs to perform a calculation of the free energy of the FFLO phase as in [14,15]. However, it will be able to tell us about the curves where the transition is second order. If the TCP coincides with the point where SN_2 meets FN_2, this also fixes the TCP which is an important feature of the phase diagram. The important way in which we extend the previous results is that we take Hartree corrections into account.

Our study differs from similar investigations reported in Refs. [22,23] in two ways. (For discussions of the phase structure of asymmetric systems at finite temperature in condensed matter systems, see [24–27].) First, we restrict our analysis to the weak coupling region and perform a self-consistent calculation of the thermodynamic properties of both the normal and the superfluid phases within the purview of mean-field theory (Hartree approximation). One drawback of this approach is that we neglect particle-hole screening which is important in the gap equation at weak coupling [28,29]. This screening is expected to reduce the gap by a factor $\simeq 2.2$. In the conclusions (Sec. IV) we will return to a discussion of how this suppression may affect our final answers. Second, we establish the region in temperature and number asymmetry where the homogeneous states are unstable with respect to small amplitude inhomogeneous perturbations.

Although our analysis is strictly valid only in the weak coupling regime, unlike earlier work, we properly account for the single particle energy shifts—or Hartree corrections—that are present both in the normal and superfluid state, in a self-consistent field-theoretic approach. We find that these corrections can change the location and shape of the phase boundaries on the phase diagram of the two component Fermi gas. We also find that a finite-temperature superfluid state is favored over the normal state at temperatures above the critical temperature for the first-order transition. In a narrow window of chemical potential asymmetry, with increasing temperature there is first a first-order transition from the superfluid to the normal phase and then at higher temperature, a second-order transition to a weakly superfluid state which exists in a limited temperature interval. In this state, finite-temperature effects that smear the Fermi surface, facilitate pairing. We will refer to this homogeneous phase as the "fragile" superfluid.

The "reentrance effect" [20], i.e., the reappearance of pairing as we increase temperature keeping the relative density asymmetry constant, was observed several years ago by [30,31] (also see [32]) who considered pairing between protons and neutrons in asymmetric nuclear matter, meaning matter consisting of unequal densities of protons and neutrons. Such an effect of temperature on pairing was also found in the context of pairing between u and d quarks in the 2SC phase [33–39]. The "reentrance effect" was found in neutral Fermi gases in [17–21], where work was done in the canonical ensemble with fixed densities of the two pairing species. In neutral Fermi systems it was generically found that these finite-temperature paired states were unstable to phase separation [16–21]. In charged systems such as nuclear and quark matter, phase separation will lead to the formation of domains of typical size equal to the Debye screening length. The stability of these states will depend on the surface tension because of the finite surface to volume ratio of these domains [40]. In contrast, the fragile superfluid state that we find when we include Hartree corrections, is stable with respect to phase separation, but as we shall show later, it is unstable with respect to gradient perturbations.

To study the gradient instabilities we expand the free energy in a Ginzburg-Landau series about the solution of the gap equation, and calculate the coefficient of the quadratic term in the order parameter as a function of its Fourier mode index. We ask the question whether this coefficient is nega-

tive for some Fourier mode(s), indicating a gradient instability. The simplest case is an expansion about the normal phase with a zero background value for the difermion condensate. In the presence of a small position-dependent condensate

$$\eta(\mathbf{r}) = \int \bar{d}^3\mathbf{k} e^{i\mathbf{k}\cdot\mathbf{r}} \eta(\mathbf{k}), \tag{1}$$

we write the change in the free energy as

$$\int \bar{d}^3\mathbf{k}[\alpha + f(|\mathbf{k}|)]\eta(\mathbf{k})\eta(-\mathbf{k}) + O(\eta^4), \tag{2}$$

where we have split the terms in a way that $f(|\mathbf{k}|)$ is zero for $\mathbf{k}=\mathbf{0}$. $\alpha<0$ points to an instability toward the formation of a homogeneous condensate while $f(|\mathbf{k}|)<0$ points to an instability toward an inhomogeneous modulation of the condensate. We find that there is a window of temperature and chemical potential splitting where the inhomogeneous superfluid phases may be favored.

The outline of the paper is as follows. We begin by writing the Lagrangian, and reviewing how to include Hartree corrections to the calculation of the gap parameter Δ and the free energy Ω of the system in Sec. II. We then proceed with the calculation of Δ and Ω in Sec. III which will let us find the phase boundary between the superfluid and the normal phase. We first consider homogeneous phases, meaning Δ independent of position, and follow with a discussion of inhomogeneous phases. We conclude with a summary of our results and discussions in Sec. IV. In the Appendix we use our expressions to calculate the polarization as a function of the distance from the center of an isotropic atomic trap, for typical trap parameters. We also identify the region where inhomogeneous phases may be found in a typical trap geometry.

II. MODEL LAGRANGIAN

We describe the gas of two species of fermions, ψ_1 and ψ_2, with chemical potentials μ_1 and μ_2, at finite temperature T, by a model Lagrangian density of the form

$$\mathcal{L} = \psi_\alpha^\dagger\{[i\partial_t - \xi(\hat{\mathbf{p}})]\delta_{\alpha\beta} + \delta\mu\sigma^z_{\alpha\beta}\}\psi_\beta + \frac{\lambda}{2}\psi_\alpha^\dagger\psi_\beta^\dagger\psi_\beta\psi_\alpha, \tag{3}$$

where $\xi(\hat{\mathbf{p}})=\hat{\mathbf{p}}^2/(2m)-\mu$ and α,β run over 1, 2. The chemical potentials for the two species of fermions, ψ_1 and ψ_2, in terms of the average chemical potential μ and the splitting $2\delta\mu$ are, $\mu_1=\mu+\delta\mu$ and $\mu_2=\mu-\delta\mu$, respectively. We are interested in the case where the interaction between the two species of fermions is attractive, meaning the coupling $\lambda>0$. In the BCS regime, then, for small enough T and $\delta\mu$, the phase of the system will be characterized by a nonzero difermion condensate

$$\langle\psi_\alpha(\mathbf{r})\psi_\beta(\mathbf{r})\rangle = \frac{1}{\lambda}\epsilon_{\alpha\beta}\Delta(\mathbf{r}). \tag{4}$$

We are interested in the phase boundary between such a superfluid phase and the normal phase, where $\Delta(\mathbf{r})=0$.

In addition, the system will be characterized by specific profiles for the number density of the two species,

$$\langle\psi_1^\dagger(\mathbf{r})\psi_1(\mathbf{r})\rangle = n_1(\mathbf{r}), \quad \langle\psi_2^\dagger(\mathbf{r})\psi_2(\mathbf{r})\rangle = n_2(\mathbf{r}). \tag{5}$$

In our calculations we will find it more convenient to write n_1 and n_2 in terms of the average density $\bar{n}(r)=(1/2)[n_1(\mathbf{r})+n_2(\mathbf{r})]$ and the difference in densities $\delta n(r)=(1/2)[n_1(\mathbf{r})-n_2(\mathbf{r})]$.

To specify the system for any T, μ, $\delta\mu$ for a given λ (which we will trade for the scattering length a), we need three equations that let us solve for the three variables Δ, $\bar{n}$, and δn. These are the gap and the number equations. For homogeneous condensates these take the form,

$$\frac{\partial\Omega}{\partial\Delta} = 0, \quad \frac{\partial\Omega}{\partial\mu} = -2\bar{n}, \quad \frac{\partial\Omega}{\partial\delta\mu} = -2\delta n. \tag{6}$$

We calculate the free energy, Ω, in an approximation where we replace the four Fermi interaction by its mean-field value,

$$\begin{aligned}\frac{\lambda}{2}&\psi_\alpha^\dagger(\mathbf{r})\psi_\beta^\dagger(\mathbf{r})\psi_\beta(\mathbf{r})\psi_\alpha(\mathbf{r}) \\ &\to \frac{1}{2}\Delta^*(\mathbf{r})\epsilon_{\alpha\beta}\psi_\alpha(\mathbf{r})\psi_\beta(\mathbf{r}) - \frac{1}{2}\Delta(\mathbf{r})\epsilon_{\alpha\beta}\psi_\alpha^\dagger(\mathbf{r})\psi_\beta^\dagger(\mathbf{r}) \\ &\quad - \frac{|\Delta(\mathbf{r})|^2}{\lambda} + \lambda n_1(\mathbf{r})\psi_2^\dagger(\mathbf{r})\psi_2(\mathbf{r}) + \lambda n_2(\mathbf{r})\psi_1^\dagger(\mathbf{r})\psi_1(\mathbf{r}) \\ &\quad - \lambda n_1(\mathbf{r})n_2(\mathbf{r}).\end{aligned} \tag{7}$$

The terms proportional to n_1 and n_2 give rise to Hartree corrections to the free energy.

Upon making the mean-field approximation, and performing standard manipulations, we can write the Lagrangian density [Eq. (3)] in a quadratic form in terms of the Nambu-Gorkov spinor,

$$\Psi = (\psi_1\ \psi_2\ \psi_1^\dagger\ \psi_2^\dagger)^T. \tag{8}$$

The final answer is

$$\begin{aligned}\mathcal{L} = \frac{1}{2}\Psi^\dagger&\begin{pmatrix} i\partial_t - \tilde{\xi}(\mathbf{p}) + \delta\tilde{\mu}\sigma^3 & -\Delta(x)\varepsilon \\ \Delta^*(x)\varepsilon & i\partial_t + \tilde{\xi}(\mathbf{p}) - \delta\tilde{\mu}\sigma^3 \end{pmatrix}\Psi + \delta(\mathbf{0})\tilde{\mu} \\ &- \frac{|\Delta|^2}{\lambda} - \lambda[\bar{n}^2(\mathbf{r}) - \delta n^2(\mathbf{r})],\end{aligned} \tag{9}$$

where $\tilde{\xi}(\mathbf{p})=\hat{\mathbf{p}}^2/(2m)-\tilde{\mu}$. $\tilde{\mu}$ and $\delta\tilde{\mu}$ include the Hartree terms and are given by

$$\tilde{\mu} = \mu + \lambda\bar{n}, \quad \delta\tilde{\mu} = \delta\mu - \lambda\delta n. \tag{10}$$

The presence of the mysterious looking term $\delta(\mathbf{0})\tilde{\mu}$ in Eq. (9) can be explained as follows.

When written in terms of the fields ψ and $\psi^\dagger$, the mean-field Lagrangian density has a piece $\Sigma_\alpha\tilde{\mu}_\alpha\psi_\alpha^\dagger\psi_\alpha$. To write this in a symmetric form in terms of the components of the Nambu-Gorkov spinor Ψ, we need to exchange the ordering of ψ and $\psi^\dagger$, which gives rise to the term in question. More explicitly,

$$\sum_\alpha \tilde{\mu}_\alpha \psi_\alpha^\dagger \psi_\alpha = \frac{1}{2}\sum_\alpha (\tilde{\mu}_\alpha \psi_\alpha^\dagger \psi_\alpha + \tilde{\mu}_\alpha \psi_\alpha^\dagger \psi_\alpha)$$

$$= \frac{1}{2}\sum_\alpha [\tilde{\mu}_\alpha \psi_\alpha^\dagger \psi_\alpha - \tilde{\mu}_\alpha \psi_\alpha \psi_\alpha^\dagger + \tilde{\mu}_\alpha \delta(\mathbf{0})], \quad (11)$$

where we have used the fermion anticommutation relation

$$\{\psi_\alpha(\mathbf{r}), \psi_\beta^\dagger(\mathbf{r}')\} = \delta_{\alpha\beta}\delta(\mathbf{r}-\mathbf{r}'). \quad (12)$$

This term is important in canceling out a divergent contribution to the free energy, as we shall see below. A similar term occurs while reordering $\Sigma_\alpha \psi_\alpha^\dagger [i\partial_t - \hat{\mathbf{p}}^2/(2m)]\psi_\alpha$, but is the same in normal and superfluid matter and does not affect the phase competition.

In the mean-field approximation the Lagrangian density is bilinear in the fermion fields and the free energy is found by direct integration over the fields. We find

$$\int d^4x_E \Omega = \int d^4x_E \left(-\delta(\mathbf{0})\tilde{\mu} + \frac{|\Delta(\mathbf{r})|^2}{\lambda} + \lambda[\bar{n}^2(\mathbf{r}) - \delta n^2(\mathbf{r})] \right) - \mathrm{Tr}\left[\ln \begin{pmatrix} -\partial_{x^4} - \tilde{\xi}(\mathbf{p}) + \delta\tilde{\mu} & -\Delta(\mathbf{r}) \\ -\Delta^*(\mathbf{r}) & -\partial_{x^4} + \tilde{\xi}(\mathbf{p}) + \delta\tilde{\mu} \end{pmatrix} \right], \quad (13)$$

where x_E represents the Euclidean space four vector $(x^4, \mathbf{r})$ with $\mathbf{r}$ lying in position space of volume V, and $x^4 \in [-1/(2T), 1/(2T)]$.

We now compare the free energies of the superfluid phases to the normal phase to find where the boundary between the phases lies.

III. PHASE BOUNDARY BETWEEN THE SUPERFLUID AND NORMAL PHASE

We first consider the competition between the homogeneous superfluid phase and the normal phase, followed by the competition between inhomogeneous superfluids and the normal phase. Finally we consider the region of the homogeneous superfluid that suffers from a current instability.

A. Homogeneous superfluid and the normal phase

The homogeneous phases are defined by the condition that Δ, $\bar{n}$, and δn are all independent of $\mathbf{r}$. The argument of the ln in Eq. (13) is then diagonal in momentum space and the free-energy density is simply

$$\Omega(\Delta, \bar{n}, \delta n, T, \mu, \delta\mu) = -\tilde{\mu}\delta(\mathbf{0}) + \frac{|\Delta|^2}{\lambda} + \lambda(\bar{n}^2 - \delta n^2) - \int d^3\mathbf{p} \left(T \sum_{\substack{p^4 = \\ (2n+1)\pi T}} \ln\{[ip^4 + \delta\tilde{\mu} - \tilde{\epsilon}(\mathbf{p})][ip^4 + \delta\tilde{\mu} + \tilde{\epsilon}(\mathbf{p})]\} \right)$$

$$= \frac{|\Delta|^2}{\lambda} + \lambda[\bar{n}^2(\mathbf{r}) - \delta n^2(\mathbf{r})] - \int d^3\mathbf{p} \left(T\left\{ \ln\left[\cosh\left(\frac{\delta\tilde{\mu} + \tilde{\epsilon}(\mathbf{p})}{2T} \right) \right] + \ln\left[\cosh\left(\frac{-\delta\tilde{\mu} + \tilde{\epsilon}(\mathbf{p})}{2T} \right) \right] \right\} + \tilde{\mu} \right), \quad (14)$$

where $\tilde{\epsilon}(\mathbf{p}) = \sqrt{\tilde{\xi}^2(\mathbf{p}) + |\Delta|^2}$ and we have rewritten $\delta(\mathbf{0})$ as an integral over momentum space.

The gap equation is the condition that the free energy is stationary with respect to small variations in the magnitude of Δ (a position independent phase of Δ does not affect the free energy and hence, for simplicity, we will take Δ to be real and positive for the rest of this section),

$$0 = \frac{\partial\Omega}{\partial\Delta} = \frac{2\Delta}{\lambda} - \frac{1}{2}\int d^3\mathbf{p} \frac{\Delta}{\tilde{\epsilon}(\mathbf{p})} \left[\tanh\left(\frac{\delta\tilde{\mu} + \tilde{\epsilon}(\mathbf{p})}{2T} \right) + \tanh\left(\frac{-\delta\tilde{\mu} + \tilde{\epsilon}(\mathbf{p})}{2T} \right) \right]. \quad (15)$$

The trivial solution, $\Delta = 0$, corresponds to the normal phase. A competing superfluid phase exists if Eq. (15) has a solution with $\Delta \neq 0$.

As it stands, the second term in Eq. (15) is linearly divergent in $\mathbf{p}$ and needs to be regularized in some manner. One way is to cut off the momentum integration at some momentum Λ, chosen to be sufficiently larger than the Fermi momentum, $k_F = \sqrt{2m\mu}$, to capture all the features of the integrand. In the weak coupling (BCS) regime, it is enough to take Λ to be several times k_F. The solution of Eq. (15) then depends on λ and Λ, but it is useful to rewrite the results in terms of a physical observable. A popular choice is to use the relation between the s-wave scattering length a, and λ.

$$\frac{1}{\lambda} = \frac{-m}{4\pi a} + \int d^3\mathbf{p} \frac{m}{\mathbf{p}^2}. \quad (16)$$

Canceling $2\Delta \neq 0$ from the right-hand side of the gap equation, Eq. (15), and substituting $1/\lambda$ in the first term in Eq. (15) from Eq. (16), we obtain the relation

$$-\frac{m}{4\pi a}=\int \bar{d}^3\mathbf{p}\left\{\frac{1}{4\tilde{\epsilon}(\mathbf{p})}\left[\tanh\left(\frac{\delta\tilde{\mu}+\tilde{\epsilon}(\mathbf{p})}{2T}\right)+\tanh\left(\frac{-\delta\tilde{\mu}+\tilde{\epsilon}(\mathbf{p})}{2T}\right)\right]-\frac{m}{\mathbf{p}^2}\right\}, \tag{17}$$

which is now cutoff independent. Recall, however, that λ also appears implicitly in the definitions of $\tilde{\mu}$ and $\delta\tilde{\mu}$ [Eq. (10)] where it multiplies $\bar{n}$ and δn, respectively. In all these places, we replace λ by $-(4\pi a)/m$. To see why this is reasonable, consider Eq. (16) with a momentum cutoff Λ,

$$\frac{1}{\lambda}=-\frac{m}{4\pi a}+m\Lambda. \tag{18}$$

If $|4\pi\Lambda a|\ll 1$, then in Eq. (18) we can ignore the second term on the right-hand side compared to the first term. In the weak coupling limit $|\pi k_F a|\ll 1$. If Λ is taken to be not many times larger than k_F, as we argued can be done in the weak coupling regime, then indeed we can take λ to be $-(4\pi a)/m$ to a good approximation.

To summarize, the gap equation is given by Eq. (17) with

$$\tilde{\mu}=\mu+\left(\frac{-4\pi a}{m}\right)\bar{n},\quad \delta\tilde{\mu}=\delta\mu-\left(\frac{-4\pi a}{m}\right)\delta n. \tag{19}$$

The number equations are found by explicitly calculating the derivatives with respect to μ and $\delta\mu$ [Eq. (6)]. The final expressions are given below,

$$-\bar{n}=\frac{1}{4}\int \bar{d}^3\mathbf{p}\left\{\left[\tanh\left(\frac{\delta\tilde{\mu}+\tilde{\epsilon}(\mathbf{p})}{2T}\right)+\tanh\left(\frac{-\delta\tilde{\mu}+\tilde{\epsilon}(\mathbf{p})}{2T}\right)\right]\frac{\tilde{\xi}(\mathbf{p})}{\tilde{\epsilon}(\mathbf{p})}-2\right\} \tag{20}$$

and

$$-\delta n=\frac{1}{4}\int \bar{d}^3\mathbf{p}\left\{\left[-\tanh\left(\frac{\delta\tilde{\mu}+\tilde{\epsilon}(\mathbf{p})}{2T}\right)+\tanh\left(\frac{-\delta\tilde{\mu}+\tilde{\epsilon}(\mathbf{p})}{2T}\right)\right]\right\}, \tag{21}$$

with $\tilde{\mu}$ and $\delta\tilde{\mu}$ given by Eq. (19).

For the normal phase, $\Delta=0$, and we can solve Eqs. (20) and (21) to find $\bar{n}$ and δn to obtain values we will call $\bar{n}_N$ and δn_N, respectively. The free energy of the normal phase is given by

$$\Omega_N(\mu,\delta\mu,T)=\left(\frac{-4\pi a}{m}\right)(\bar{n}_N^2-\delta n_N^2)-\int \bar{d}^3\mathbf{p}\left(T\left\{\ln\left[\cosh\left(\frac{\delta\tilde{\mu}_N+\tilde{\xi}(\mathbf{p})_N}{2T}\right)\right]+\ln\left[\cosh\left(\frac{-\delta\tilde{\mu}_N+\tilde{\xi}(\mathbf{p})_N}{2T}\right)\right]\right\}+\tilde{\mu}_N\right) \tag{22}$$

with $\tilde{\xi}(\mathbf{p})_N=\hat{\mathbf{p}}^2/(2m)-\tilde{\mu}_N$ and

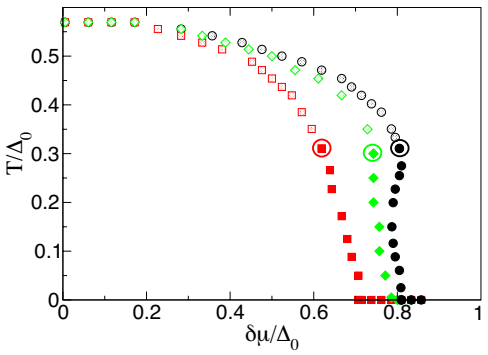

FIG. 2. (Color online) We show the phase boundary between normal and homogeneous superfluid phases in $\delta\mu,T$ space, for $g=-0.72$. In the curve marked by circles (black), we include the Hartree corrections. The value of Δ_0/μ is 0.058. The curve marked by squares (red) does not include Hartree corrections. The value of Δ_0/μ in this case is 0.03. This curve (but of course not the value of Δ_0/μ) coincides with the $g\to-\infty$ limit of the curve which includes the Hartree corrections, because we have scaled out Δ_0. At $T=0$, the first-order phase transition from the superfluid to the normal phase occurs at $\delta\mu/\Delta_0\sim 0.71$, consistent with weak coupling results. We also show the curve (including Hartree) at a smaller value of the coupling where $g=-1.06$, with diamonds (green). The value of Δ_0/μ for this value of g is 0.0097. The filled points mark the region where the phase transition is first order while the hollow points mark a second-order transition. The points where the transition changes from being second order to becoming first order have been circled.

$$\tilde{\mu}_N=\mu+\left(\frac{-4\pi a}{m}\right)\bar{n}_N,\quad \delta\tilde{\mu}_N=\delta\mu-\left(\frac{-4\pi a}{m}\right)\delta n_N. \tag{23}$$

If, in addition, Eqs. (17), (20), and (21) possess solutions with $\Delta\neq 0$, $\bar{n}$ and δn, we need to compare the free energies of these superfluid solutions Ω_s to Ω_N. The difference in the free energies is given by

$$\begin{aligned}(\Omega_s-\Omega_N)(\mu,\delta\mu,T)&=-\frac{m\Delta^2}{4\pi a}+\left(\frac{-4\pi a}{m}\right)(\bar{n}^2-\bar{n}_N^2-\delta n^2+\delta n_N^2)\\&\quad-\int \bar{d}^3\mathbf{p}\left(T\left\{\ln\left[\cosh\left(\frac{\delta\tilde{\mu}+\tilde{\epsilon}(\mathbf{p})}{2T}\right)\right]+\ln\left[\cosh\left(\frac{-\delta\tilde{\mu}+\tilde{\epsilon}(\mathbf{p})}{2T}\right)\right]\right\}\right.\\&\quad\left.-T\left\{\ln\left[\cosh\left(\frac{\delta\tilde{\mu}_N+\tilde{\xi}(\mathbf{p})_N}{2T}\right)\right]+\ln\left[\cosh\left(\frac{-\delta\tilde{\mu}_N+\tilde{\xi}(\mathbf{p})_N}{2T}\right)\right]\right\}+\tilde{\mu}-\tilde{\mu}_N-\frac{m\Delta^2}{\mathbf{p}^2}\right).\end{aligned} \tag{24}$$

If $\Omega_s-\Omega_N>0$ then the normal phase is favored over the superfluid phase, and vice versa. In Fig. 2 we look at the boundary marking the normal to superfluid phase transition

in $T, \delta\mu$ space for $g=(\pi k_F a)^{-1}=-0.72$. For different values of μ and m, if we choose a so that the dimensionless parameter g remains the same, then the physical quantities scale with μ and m as follows:

$$n_\alpha[m,\mu,T,\delta\mu] = m^{3/2}\mu^{3/2} n_\alpha[1,1,(T/\mu),(\delta\mu/\mu)],$$

$$\Delta[m,\mu,T,\delta\mu] = \mu\Delta[1,1,(T/\mu),(\delta\mu/\mu)],$$

$$\Omega[m,\mu,T,\delta\mu] = m^{3/2}\mu^{5/2}\Omega[1,1,(T/\mu),(\delta\mu/\mu)]. \quad (25)$$

In particular, the value of Δ_0, the value of the gap parameter at $T=0$ and $\delta\mu=0$, scales linearly with μ. To remove the dependence of the phase transition curve on the overall scales, it is useful to draw the phase diagram in terms of dimensionless variables. Since Δ_0 is proportional to μ, we take the x axis to be $\delta\mu/\Delta_0$ and the y axis to be T/Δ_0.

For comparison, in Fig. 2 we also show the result when one does not include the Hartree corrections. One effect of Hartree corrections is to simply shift the chemical potentials. For example, at $T=0$ and $\delta\mu=0$, including these increases the "effective" chemical potential, $\tilde{\mu}=\mu-(4\pi a/m)\bar{n}$. (Recall that $a<0$ in the BCS regime.) Therefore, for the same a, the value of Δ_0 is greater when we include the Hartree corrections, compared to when we do not include them. For example, for $g=-0.72$, $\Delta_0/\mu=0.03$ if we do not include the Hartree corrections, while $\Delta_0/\mu=0.058$ when we include them. To get rid of this overall change in Δ_0, we scale T and $\delta\mu$ in the "non-Hartree" curve by the "non-Hartree" value of Δ_0. The two curves are still different, and that has to do with the fact that including Hartree corrections affects the competition between the normal and the superfluid phases. Number densities, and therefore Hartree corrections, are different in the two phases at the phase boundary, if the phase transition between the two phases is first order. In the following paragraphs, we discuss the effect of Hartree corrections on the phase transition curve between the normal and the superfluid phase in more detail.

First, looking along the y axis, at $\delta\mu=0$, the transition from the superfluid to the normal phase at the critical temperature is second order, and the number densities in the two phases are the same at the critical temperature. It is understandable, therefore, that the transition occurs at $T_c/\Delta_0 \sim 0.567$, the standard weak coupling value. For zero $\delta\mu$, therefore, we see that the effect of Hartree corrections in weak coupling can be taken into account by simply shifting of the chemical potentials, to their "renormalized" value. The key is that this is not true for $\delta\mu \neq 0$.

Next, looking at $T=0$, $\delta\mu/\Delta_0$ at the first-order transition is larger than the weak coupling value 0.707, as pointed out earlier in [6]. Since at $T=0$, $\delta n=0$ in the superfluid phase (the superfluid phase is gapped), this is not simply due to a reduction in the effective splitting between the Fermi surfaces in the superfluid region ($\delta\tilde{\mu}=\delta\mu \sim 0.81\Delta_0$ for the superfluid phase at the phase transition). As discussed above, the change is due to the fact that $\bar{n}$ and δn change abruptly at the first-order phase boundary. More specifically, there are two effects both of which drive the phase transition to larger $\delta\mu$. First, δn is positive in the normal phase, implying $\delta\tilde{\mu}$ is smaller than $\delta\mu$, which increases the free energy of the normal phase. Second, $\bar{n}$ is larger in the superfluid phase because of pairing, and this also makes the superfluid phase more favorable.

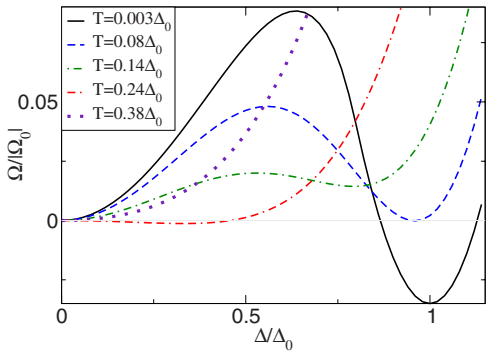

FIG. 3. (Color online) The free energy as a function of Δ at $\delta\mu/\Delta_0=0.795$ for various values of T. The solid curve (black) corresponds to the lowest temperature, $T/\Delta_0=0.003$, and clearly shows a robust superfluid phase with $\Delta \sim \Delta_0$. The dashed curve (blue) corresponds to $T/\Delta_0=0.08$ and is the point of a first-order phase transition to the normal phase. A "fragile" superfluid phase reappears before it disappears again at a higher temperature.

Things are interesting close to $\delta\mu/\Delta_0 \sim 0.8$, where the shape of the curve is qualitatively altered. For a window of splittings, $\delta\mu/\Delta_0 \in (0.79, 0.81)$, as we increase the temperature, we encounter not one but three normal-superfluid transitions. To clarify how this comes about, consider the shape of Ω as a function of Δ for various values of the temperature, at $\delta\mu/\Delta_0=0.795$ (Fig. 3). At $T=0$, the local minimum at $\Delta=\Delta_0$ is favored. As we increase the temperature, this minimum becomes shallower and eventually there is a first-order transition to the normal phase. As we keep increasing the temperature, the $\Delta=0$ solution becomes unstable and the superfluid state is favored again for a range of temperatures. Eventually, at a large enough temperature, there is a second-order transition to the normal phase. This reappearance of superfluidity at higher temperatures can be understood intuitively as follows. At zero temperature, BCS pairing is stressed due to a nonzero $\delta\mu$, because fermions of the two species cannot find partners of opposite momenta lying on the distinct Fermi surfaces determined by their different chemical potentials. BCS pairing in such systems requires the two distinct Fermi spheres to equalize at a Fermi momentum different from the value given by the corresponding chemical potentials, costing free energy. At nonzero temperatures, however, the Fermi surfaces are smeared and it is possible to find partners of opposite momenta even without equalizing the Fermi surfaces.

To see in a different way why there are three transitions, it is useful to expand the free energy in powers of Δ^2 (Ginzburg-Landau expansion) and look at how the coefficient of the quadratic term changes as we change T, keeping $\delta\mu$ constant. We write the free energy as $\alpha\Delta^2+O(\Delta^4)$. $\alpha<0$ points to an instability in the $\Delta=0$ state to the formation of a nonzero condensate, while $\alpha>0$ means that the normal state is locally stable, but does not tell us whether it is globally favored or not.

In Fig. 4 we plot α (in units of Δ_0^2) as a function of T/Δ_0, for $\delta\mu=0.795\Delta_0$ kept constant. For small T, the normal

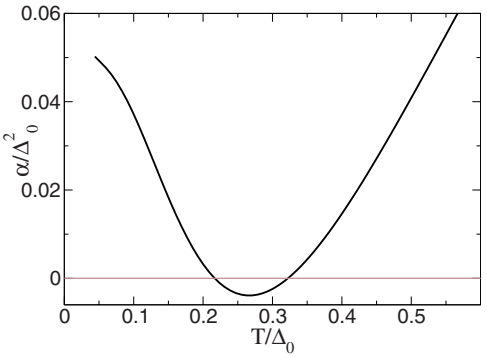

FIG. 4. (Color online) Plot of α as a function of T/Δ_0 for $\delta\mu = 0.795\Delta_0$. The normal phase is locally stable for $T/\Delta_0 \in (0, 0.22)$, locally unstable for $T/\Delta_0 \in (0.22, 0.33)$, and locally stable for T larger than $0.33\Delta_0$.

phase is locally stable, but globally disfavored to the $\Delta=\Delta_0$ state (Fig. 3). As we increase T, the superfluid phase becomes less and less favorable until finally at $T/\Delta_0=0.08$ the normal phase is globally favored. On increasing T further, we find that the normal phase becomes locally unstable in the region $T/\Delta_0 \in (0.22, 0.33)$, and this gives rise to a region of "fragile" superfluidity.

In the limit $g \to \infty$, the effect of the Hartree corrections on the chemical potentials tends to zero and therefore in this limit the normal to superfluid phase transition curve in Fig. 2 is the same as that without Hartree corrections (red). As we increase the coupling, the phase transition moves towards the right, meaning that the transition from superfluid to the normal phase occurs at larger values of $\delta\mu$, as the Hartree corrections become more important. We see that in addition, the transition curve develops the phenomenon of reentrance. This discussion applies only in the weak coupling regime. As we shall discuss in Sec. IV, for large enough coupling, the effect of the Hartree corrections is expected to saturate.

B. Inhomogeneous condensates

Let us now consider the case where Δ, $\bar{n}$, and δn depend on $\mathbf{r}$. The argument of the ln in Eq. (13) is no longer diagonal in momentum space and hence we evaluate the free energy in a Ginzburg-Landau expansion. We are interested in finding the curve along which the normal phase becomes unstable to the growth of an inhomogeneous condensate. Working in the limit of small $\Delta(\mathbf{r})$, we expand the ln in $\Delta(\mathbf{r})$ and drop terms proportional to Δ^4 and higher, and obtain

$$\int d^3\mathbf{r}\Omega[\Delta(\mathbf{r})] = \int d^3\mathbf{r}\left(-\tilde{\mu}\delta(\mathbf{0}) + \frac{|\Delta(\mathbf{r})|^2}{\lambda} + \lambda(\bar{n}^2 - \delta n^2)\right) - T \times \sum_{p^4=(2n+1)\pi T} [\mathrm{Tr}_{\mathbf{r}}(\ln\{[ip^4 + \delta\tilde{\mu} - \tilde{\xi}(\mathbf{p})] \times [ip^4 + \delta\tilde{\mu} + \tilde{\xi}(\mathbf{p})]\}) - \mathrm{Tr}_{\mathbf{r}}\{[ip^4 + \delta\tilde{\mu} - \tilde{\xi}(\mathbf{p})]^{-1}\Delta(\mathbf{r}) \times [ip^4 + \delta\tilde{\mu} + \tilde{\xi}(\mathbf{p})]^{-1}\Delta^*(\mathbf{r})\}]. \quad (26)$$

We now argue that within the approximations we are working, we can replace $\bar{n}$ and δn by their values in normal matter to compute Ω. It is obvious that we can do so in the term,

$$T \sum_{p^4=(2n+1)\pi T} \{[ip^4 + \delta\tilde{\mu} - \tilde{\xi}(\mathbf{p})]^{-1}\Delta(\mathbf{r}) \times [ip^4 + \delta\tilde{\mu} + \tilde{\xi}(\mathbf{p})]^{-1}\Delta^*(\mathbf{r})\}, \quad (27)$$

because the corrections to $\bar{n}$ and δn due to pairing are proportional to Δ^2, and keeping these corrections in Eq. (27) (where they appear in $\tilde{\mu}$ and $\delta\tilde{\mu}$) will only change the result by order Δ^4. There are $O(\Delta^2)$ contributions to Ω from $\tilde{\mu}\delta(\mathbf{0})$, $\lambda(\bar{n}^2 - \delta n^2)$, and $\mathrm{Tr}_{\mathbf{r}}(\ln\{[ip^4 + \delta\tilde{\mu} - \tilde{\xi}(\mathbf{p})][ip^4 + \delta\tilde{\mu} + \tilde{\xi}(\mathbf{p})]\})$, but in all these cases, the Δ^2 correction to $\bar{n}$ or δn is further multiplied by λ and for weak coupling, this should give a small overall contribution. (This is the Δ^2 correction to the Hartree term which itself is a correction.) In the approximation where we neglect this contribution, when we calculate the difference between the normal and superfluid free energies, these three terms cancel out and we obtain

$$\int d^3\mathbf{r}\{\Omega[\Delta(\mathbf{r})] - \Omega_N\} = \int d^3\mathbf{r}\left(\frac{|\Delta(\mathbf{r})|^2}{\lambda}\right) + \int \bar{d}^3\mathbf{p}\left(T \sum_{p^4=(2n+1)\pi T} \mathrm{Tr}_{\mathbf{r}}\{[ip^4 + \delta\tilde{\mu}_N - \tilde{\xi}(\mathbf{p})_N]^{-1}\Delta(\mathbf{r})[ip^4 + \delta\tilde{\mu}_N + \tilde{\xi}(\mathbf{p})_N]^{-1}\Delta^*(\mathbf{r})\}\right). \quad (28)$$

In momentum space this gives

$$\int d^3\mathbf{r}\{\Omega[\Delta(\mathbf{r})] - \Omega_N\} = \int \bar{d}^3\mathbf{k}\Delta(\mathbf{k})\Delta^*(-\mathbf{k}) \times \left[\frac{-m}{4\pi a} + \int \bar{d}^3\mathbf{p}\left(\frac{m}{\mathbf{p}^2} + T \sum_{p^4=(2n+1)\pi T} [ip^4 + \delta\tilde{\mu}_N - \tilde{\xi}(\mathbf{p}+\mathbf{k})_N]^{-1}[ip^4 + \delta\tilde{\mu}_N + \tilde{\xi}(\mathbf{p})_N]^{-1}\right)\right], \quad (29)$$

where we have used Eq. (16) to rewrite λ.

It is convenient at this point, to separate the "potential" contribution (the contribution independent of $\mathbf{k}$) from the "gradient" contribution (zero for $\mathbf{k}=\mathbf{0}$) [41]. We write

$$\int d^3\mathbf{r}\{\Omega[\Delta(\mathbf{r})] - \Omega_N\} = \int \bar{d}^3\mathbf{k}\Delta(\mathbf{k})\Delta^*(-\mathbf{k})[\alpha + f(|\mathbf{k}|)] \quad (30)$$

with

$$\alpha = -\frac{m}{4\pi a} + \int \bar{d}^3\mathbf{p}\left(\frac{m}{\mathbf{p}^2} + T\sum_{p^4=(2n+1)\pi T}[ip^4 + \delta\tilde{\mu}_N - \tilde{\xi}(\mathbf{p})_N]^{-1}[ip^4 + \delta\tilde{\mu}_N + \tilde{\xi}(\mathbf{p})_N]^{-1}\right)$$
$$= -\frac{m}{4\pi a} + \int \bar{d}^3\mathbf{p}\left\{\frac{m}{\mathbf{p}^2} - \left[\tanh\left(\frac{\delta\tilde{\mu}_N + \tilde{\xi}(\mathbf{p})_N}{2T}\right) + \tanh\left(\frac{-\delta\tilde{\mu}_N + \tilde{\xi}(\mathbf{p})_N}{2T}\right)\right]\frac{1}{4\xi(\mathbf{p})_N}\right\} \quad (31)$$

and

$$f(|\mathbf{k}|) = \frac{1}{2}\int \bar{d}^3\mathbf{p}\left(T\sum_{p^4=(2n+1)\pi T}\frac{[\tilde{\xi}(\mathbf{p}+\mathbf{k})_N - \tilde{\xi}(\mathbf{p})_N]^2}{\{(ip^4 + \delta\tilde{\mu}_N)^2 - [\tilde{\xi}(\mathbf{p})_N]^2\}\{(ip^4 + \delta\tilde{\mu}_N)^2 - [\tilde{\xi}(\mathbf{p}+\mathbf{k})_N]^2\}}\right)$$
$$= \frac{1}{2}\int \bar{d}^3\mathbf{p}\left[\frac{[\tilde{\xi}(\mathbf{p}+\mathbf{k})_N - \tilde{\xi}(\mathbf{p})_N]}{[\tilde{\xi}(\mathbf{p}+\mathbf{k})_N + \tilde{\xi}(\mathbf{p})_N]}\left(\frac{g[\tilde{\xi}(\mathbf{p})_N]}{\tilde{\xi}(\mathbf{p})_N} - \frac{g[\tilde{\xi}(\mathbf{p}+\mathbf{k})_N]}{\tilde{\xi}(\mathbf{p}+\mathbf{k})_N}\right)\right], \quad (32)$$

where

$$g(\xi) = \frac{1}{2}\left[\tanh\left(\frac{\delta\tilde{\mu} + \xi}{2T}\right) + \tanh\left(\frac{-\delta\tilde{\mu} + \xi}{2T}\right)\right]. \quad (33)$$

At any given temperature, for large enough $\delta\mu$, the normal phase will be favored over a phase with nonzero $\Delta(\mathbf{k})$, and the combination $\alpha+f(k)$ will be positive for all values of $k=|\mathbf{k}|$. As we decrease $\delta\mu$ keeping T constant, $\alpha+f(k)$ may become zero, and then negative, for a single mode with momentum $k=k_{\min}$. If $k_{\min}\neq 0$, this point symbolizes the onset of the instability toward the formation of an inhomogeneous condensate. At lower $\delta\mu$, more momentum modes may become unstable. If the transition from normal to inhomogeneous superfluidity is actually first order, then we expect it to occur for values of $\delta\mu$ larger than the value we find using this second-order analysis.

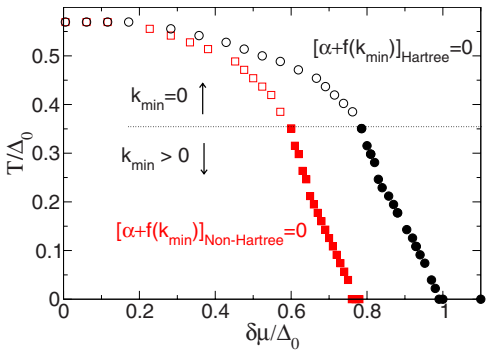

FIG. 5. (Color online) We show the curve marking a second-order phase transition between normal and inhomogeneous superfluid phases in $\delta\mu, T$ space, for $g=-0.72$. In the curve marked by circles (black), we include the Hartree corrections while the curve marked by squares (red) does not include these. Where the symbols are hollow, the value of k at which $\alpha+f(k)$ becomes zero, is zero, meaning that the instability is toward the formation of homogeneous condensates. It is reasonable that at smaller $\delta\mu$ and larger temperatures, the formation of homogeneous condensates is favored because the Fermi surface is smeared out and it is no longer advantageous to form Cooper pairs with nonzero net momenta.

Figure 5 shows the curve in $T, \delta\mu$ space, which tells us the value of $\delta\mu$ where the coefficient $\alpha+f(k)$ becomes zero for some k, as we decrease $\delta\mu$ from a large value keeping T constant. Since we are looking at a second-order phase transition line, once we take into account the shift in the chemical potentials due to the Hartree corrections, the results are consistent with the well-known results for weak coupling. For example, at $T=0$, the value of $\delta\tilde{\mu}=\delta\mu-(-4\pi a/m)\delta n$ at the phase transition is given by $\delta\tilde{\mu}/\Delta_0\sim 0.75$. Weak coupling Ginzburg-Landau calculations tell us that the transition should occur at $\delta\mu^*=0.754\Delta_0$ with the most unstable momentum $k_{\min}$ given by $v_F k_{\min}/2=1.2\delta\mu^*$. We find that the value of k which becomes unstable at $\delta\tilde{\mu}/\Delta_0\sim 0.75$ satisfies $v_F k_{\min}/2\sim 1.24\delta\tilde{\mu}$. For reference we also show the FFLO boundary excluding the Hartree corrections marked by squares (red). The instability toward inhomogeneous condensates at $T=0$ develops at $\delta\mu/\Delta_0\sim 0.75$, and the value of $v_F k_{\min}/2$ we find at this point is $1.37\delta\mu$.

C. Current instability in the homogeneous superfluid phase

In the following, we analyze the stability of the "fragile" superfluid to fluctuations that depend on position and are purely imaginary for real Δ. That is, we consider a condensate of the form

$$\langle\psi_\alpha(\mathbf{r})\psi_\beta(\mathbf{r})\rangle = \frac{1}{\lambda}\epsilon_{\alpha\beta}[\Delta + i\eta(\mathbf{r})], \quad (34)$$

where Δ and η are both real. The reason for considering purely imaginary fluctuations [Eq. (34)] is that it is clear from the free energy curve at $T=0.24\Delta_0$ in Fig. 3 that the free energy is at a local minimum at the mean-field value Δ, meaning that the system is stable to spatially uniform variation in the magnitude of the condensate. One could potentially consider position-dependent fluctuations in the magnitude of the condensate but we only consider real $\eta(\mathbf{r})$ in Eq. (34), which is related to position-dependent fluctuations in the phase of the condensate. The effective potential describing the dynamics of η can be found in a Ginzburg-Landau expansion in the same way as was done in Sec. III B, where

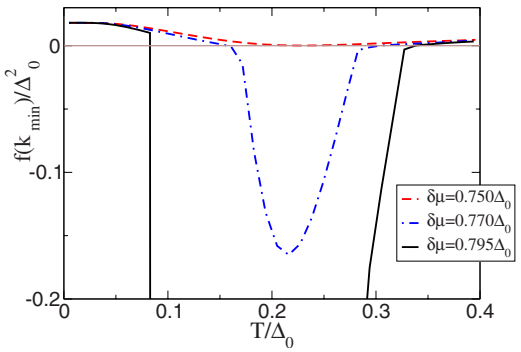

FIG. 6. (Color online) $f(\mathrm{k}_{\mathrm{min}})$ as a function of T at three values of $\delta\mu$, $\delta\mu=0.750\Delta_0$, $\delta\mu=0.770\Delta_0$, and $\delta\mu=0.795\Delta_0$. We take $g=-0.72$ as before. Looking first at $\delta\mu=0.795\Delta_0$, $f(\mathrm{k}_{\mathrm{min}})$ is clearly negative in the normal region, corresponding to $T/\Delta_0 \in (0.08, 0.22)$. It is also negative in the "fragile" superfluid region lying in $T/\Delta_0 \in (0.22, 0.33)$. Now considering $\delta\mu=0.770\Delta_0$, we find that the homogeneous condensate is unstable in $T/\Delta_0 \in (0.16, 0.29)$. Finally, for $\delta\mu=0.750\Delta_0$ (and lower), we find that the homogeneous condensate is stable for all T. These three curves form the basis of the thick dashed lines (blue) in Fig. 7.

we considered inhomogeneous fluctuations about the normal phase. The only difference now is that the background has a nonzero condensate value, Δ. The final answer has the form

$$\int d^3\mathbf{r}\{\Omega[\Delta(\mathbf{r})] - \Omega_N\} = \int \bar{d}^3\mathbf{k}\,\eta(\mathbf{k})\,\eta(-\mathbf{k})[f_\Delta(|\mathbf{k}|)] \tag{35}$$

with

$$f_\Delta(|\mathbf{k}|) = \frac{1}{4}\int \bar{d}^3\mathbf{p}\left[\frac{[\tilde{\xi}(\mathbf{p}+\mathbf{k}) - \tilde{\xi}(\mathbf{p})]^2}{[\tilde{\epsilon}(\mathbf{p}+\mathbf{k})^2 - \tilde{\epsilon}(\mathbf{p})^2]} \times\left(\frac{g[\tilde{\epsilon}(\mathbf{p})]}{\tilde{\epsilon}(\mathbf{p})} - \frac{g[\tilde{\epsilon}(\mathbf{p}+\mathbf{k})]}{\tilde{\epsilon}(\mathbf{p}+\mathbf{k})}\right)\right]. \tag{36}$$

The form in Eq. (35) closely resembles the form in Eq. (30), except now $\alpha=0$, which can be easily understood as the consequence of the fact that a position independent fluctuation in the phase of the condensate cannot change the free energy.

In Fig. 6 we plot the minimum value of $f_\Delta(k)$ (minimized over $k=|\mathbf{k}|$) as a function of T at $\delta\mu/\Delta_0=0.795$, 0.770, and 0.750 for $g=-0.72$. For $\delta\mu/\Delta_0=0.795$, we see that the minimum value, $f(k_{\mathrm{min}})$, is negative in the "fragile" superfluid region lying in $T/\Delta_0 \in (0.22, 0.33)$, indicating that it is unstable with respect to developing a position-dependent phase modulation. We see that as we decrease $\delta\mu$, the range of T where the homogeneous superfluid is unstable shrinks and for $\delta\mu/\Delta_0 < 0.750$ the homogeneous superfluid region becomes stable for all T, as it should.

The unstable region is the region of the phase diagram where the homogeneous superfluid phase is expected to be supplanted by a FFLO-like phase. We use the results of Fig. 6 below to exclude the part of the homogeneous superfluid region which is unstable.

IV. CONCLUSIONS

We calculated the effect of Hartree corrections on the phase transition curve separating the normal from the superfluid phase in the $(T, \delta\mu)$ plane, in the BCS regime.

Our analysis is similar in spirit to the calculations performed by the authors of [23], who however concentrate on the unitary regime. We work in the BCS regime, where the Hartree corrections can be calculated self-consistently, as described above. To understand the relation between the two calculations we rewrite the Hartree corrections in Eq. (19) following the notation of [23], as, $\tilde{\mu}_\sigma = \mu_\sigma - \Sigma_\sigma$ where

$$\Sigma_\sigma = \frac{4\pi a}{m} n_{-\sigma}. \tag{37}$$

This can be seen as a weak coupling limit of a formula that interpolates between the weak coupling and the unitarity regimes [42],

$$\Sigma_\sigma = \frac{4\pi}{m}\frac{a}{1-\gamma p_F a} n_{-\sigma}, \tag{38}$$

where $p_F=(6\pi^2 n)^{3/2}$ and γ is a dimensionless parameter. For $p_F a \to 0$, we get back Eq. (37). The value of γ is chosen so that the solutions of mean-field equations reproduce the relation between the density and the chemical potential found using Monte Carlo simulations, $\mu=(1+\beta)p_F^2/(2m)$, which gives $\gamma=4/[3\pi(\beta_{\mathrm{BCS}}-\beta)\sqrt{1+\beta_{\mathrm{BCS}}}] \simeq 5.350$ for the calculated values, $\beta \simeq -0.59$ and $\beta_{\mathrm{BCS}} \simeq -0.48$. At unitarity then [23],

$$\Sigma_\sigma \simeq \frac{-2.35}{m}\sqrt{\frac{1}{2m\tilde{\mu}}} n_{-\sigma}. \tag{39}$$

From the interpolating formula it is clear that for a given density, the effect of the Hartree corrections on the phase diagram increases linearly with the scattering length, as long as $p_F a \lesssim 1/\gamma$. As $p_F a$ increases beyond this value, the Hartree corrections stop increasing with a. It would be interesting in future work to use the interpolating formula, Eq. (38), over the whole range of interaction strengths to see how the Hartree corrections change as we go from weak coupling to strong coupling.

Furthermore, we considered the instability of the homogeneous states with respect to the formation of inhomogeneous condensates. The phase transition between the normal and the FFLO phases was considered in detail by Combescot and Mora in a series of papers [13–15]. In [13], the authors consider a Ginzburg-Landau expansion of the free energy around the TCP, which we write in shorthand as

$$\Omega(\Delta) = \sum_k \Delta_k^2\left(a_0 - \frac{a_2}{3}k^2 + \frac{a_4}{5}k^4\right) - \frac{1}{2}\Delta_k^4\left(\frac{a_2}{2} - \frac{a_4}{6}k^2\right) + \frac{3a_4}{8}\Delta_k^6 + O(\Delta^8, k^6). \tag{40}$$

Our expression for Ω [Eq. (30)], $\Omega=\Sigma_k[\alpha+f(k)]\Delta_k^2+O(\Delta_q^4)$, is a generalization of the second-order term in Δ [Eq. (40)], where we consider arbitrarily high powers in k. In principle, this will shift the TCP so that it no longer lies at the point

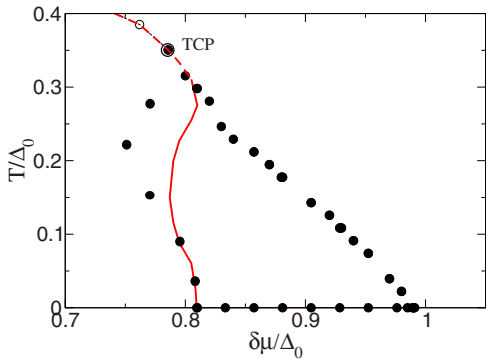

FIG. 7. (Color online) We show the phase boundaries between the normal and the inhomogeneous superfluid phases and the normal and the homogeneous superfluid phase, for $g=-0.72$. The curve that ends at $\delta\mu/\Delta_0 \sim 0.81$ (red) represents the curve where the free energies of the homogeneous phase and the normal phase are equal. The region enclosed by the curve joining the filled dots (black) marks the region where the mean-field solution is unstable toward inhomogeneity. This region is where FFLO-like phases may exist. The TCP is marked by a hollow circle (black).

where SN_1 meets SN_2 (Fig. 1). But it turns out that the shift in the TCP is small and hence we verify that a quartic expansion in k is sufficient to locate the TCP. In [14,15], the authors use a quasiclassical expansion to calculate the free energy of the FFLO phase which allows them to map out the first-order boundary between the normal and the FFLO phase. We do not calculate the first-order boundary between the normal and the superfluid phase. On the other hand, we do consider small fluctuations about the homogeneous superfluid phase and are therefore sensitive to the second-order boundary between the FFLO and the homogeneous superfluid phase (SF_2).

Our main results are shown in Figs. 2, 5, and 6 for $g=-0.72$.

First, we find that the shape of the curve marking the transition from the homogeneous superfluid phase to the normal phase, is qualitatively altered (Fig. 2). For a narrow range of $\delta\mu$ near the first-order transition, we encounter three normal-superfluid transitions as we increase the temperature keeping $\delta\mu$ constant. There is a first-order phase transition from the superfluid to the normal phase at a low temperature. As we increase the temperature, a "fragile" superfluid phase, where pairing is assisted by a temperature induced smearing of the Fermi surfaces, reappears in a window of temperatures. This is reminiscent of the "reappearance effect" found by [18–21] in a canonical ensemble where the densities of the two species are kept fixed. However, our findings are qualitatively different from these studies in that the "fragile" superfluid state is stable with respect to phase separation, and is seen only when Hartree corrections are included. However, as we discussed in Sec. III C, a region of the "fragile" state is unstable to the growth of inhomogeneous fluctuations in the phase of the condensate [18]. In Fig. 7, we zoom in on the large $\delta\mu$ region of Figs. 2 and 5 and show the homogeneous-normal and inhomogeneous-normal phase boundaries on the same diagram. The curve that meets the x axis at $\delta\mu \sim 0.81\Delta_0$ (red) represents the points where the free energies of the homogeneous superfluid and the normal phase are equal and marks the homogeneous-normal phase boundary. This boundary is superceded by the FFLO phase, because as shown above, there are parts of the homogeneous phase as well as the normal phase, that are unstable to growth of inhomogeneous fluctuations. The region enclosed by the curve joining the dots (black), shows the parameter values for which the coefficient of the $\eta(\mathbf{k})^2$ term in a Ginzburg-Landau expansion, where η is the fluctuation about the mean-field solution, becomes negative for some value of $k=k_{\min}$. This signals an instability toward the formation of an inhomogeneous condensate. Our second conclusion is that at weak coupling, Hartree corrections do not destroy the parameter space where FFLO-like phases may exist.

If this mean-field picture is taken as it is (and ignoring the inhomogeneous phases for a moment), this structure of the phase diagram could be observed in cold-atomic traps. As we go away from the center of the trap, the effective chemical potential and therefore Δ_0 decrease. Since T and $\delta\mu$ are constant across the trap, this implies that T/Δ_0 and $\delta\mu/\Delta_0$ increase. The "fragile" superfluid region can be probed by tuning the parameters, namely the number of the two species in the trap N_1 and N_2, the scattering length a, and the temperature T, so that for a given trap geometry, we pass through the "fragile" superfluid region as we go from the center of the trap to the outside.

In the Appendix, we plot profiles of the polarization $p=(n_1-n_2)/(n_1+n_2)$ as a function of r, where r is the distance from the center of the trap and n_1 and n_2 are the number densities of the two species.

While we have marked the boundaries where the homogeneous state is unstable to the growth of inhomogeneities in Fig. 8 in the Appendix, we must mention the following caveat. We have assumed the densities in the resulting inhomogeneous phase is approximately the same as the density in the background homogeneous phase. For a more accurate determination of the polarization profiles, we will need to calculate the number densities of the two species in an inhomogeneous condensate more accurately than we have done above. Such a calculation without including self-energy corrections was performed in [14] whose results suggest that there is a significant change in the density at the phase border between the FFLO and the normal phase. If this result persists when self-energy corrections are included, a sharp change in density will be useful in locating the FFLO to normal phase transition in the trap. We leave an extension of this calculation to include Hartree corrections, for future work.

Another issue that warrants further investigation is the role of polarization effects (also known as the Gorkov-Barkhudarov corrections) that can reduce the gap. In weak coupling, medium polarization results in screening of the interactions and reduces the gap and the critical temperature by a factor of $(4e)^{1/3} \sim 2.2$ when $\delta\mu=0$ [28,29]. For weak coupling, this screening effect is essentially independent of T and $\delta\mu$ in the superfluid phase. If we were to incorporate this screening by modifying the four-fermion coupling in the pairing channel to obtain the Gorkov suppression at $T=0$ and $\delta\mu=0$, one can argue (and we have verified by a detailed

calculation) that the phase boundary is simply scaled by the same reduction factor 2.2 both in T and $\delta\mu$. Since Δ_0 is also scaled down by exactly the same factor, the phase transition curve (shown in Fig. 2) will not be affected by including the screening corrections. However, a systematic calculation of these medium effects at moderate coupling is challenging and preliminary investigations suggest that the gap at $T=0$ and $\delta\mu=0$ is not as strongly suppressed (see [43]). Furthermore, at moderate coupling the dependence of the screening on T and $\delta\mu$ cannot be neglected while drawing the phase diagram. We leave a systematic calculation of how Gorkov corrections evolve with coupling strength, T and $\delta\mu$ for future work.

Despite these caveats, we reiterate that our investigation points to several interesting qualitative features that arise only when Hartree corrections are included. In particular we see that the region in phase diagram susceptible to gradient instabilities is moderately enhanced by these corrections. The shape of the normal-superfluid phase boundary is shown to depend on the nature of these mean-field energy shifts since they differ in the two phases in the vicinity of the first-order transition. In particular the Clogston-Chandrashekar point, which is given by $\delta\mu=\Delta/\sqrt{2}$, is shifted to higher values of $\delta\mu$ by these corrections.

ACKNOWLEDGMENTS

R.S. thanks Krishna Rajagopal for discussions and suggestions. The authors also acknowledge discussions with Michael Forbes, Joe Carlson, Mark Alford, and Alex Gezerlis. The authors also thank an anonymous referee for valuable suggestions. This research was supported by the Department of Energy under Contract No. W-7405-ENG-36 and by the LANL/LDRD Program.

APPENDIX: A HARMONIC TRAP TUNED TO PASS THROUGH THE FRAGILE REGION

In Fig. 8, we plot profiles of the polarization $p=(n_1-n_2)/(n_1+n_2)$ as a function of r, where r is the distance from the center of the trap and n_1 and n_2 are the number densities of the two species. The trap is taken to be spherically symmetric, with a harmonic trapping angular frequency $\omega=100$ Hz [8–12]. The harmonic potential can be written as $V(r)=\frac{1}{2}\hbar\omega(r/r_0)^2$ with $r_0=\sqrt{\hbar/(m\omega)}$, where m is the mass of ^{6}Li atoms. In natural units, $\omega=4.127\times10^{-13}$ eV, $m=5.61\times10^{+9}$ eV, and $r_0=20.783$ eV^{-1}.

With the geometry of the trap specified, we now try to tune the parameters of the experiment $\bar{N}=(N_1+N_2)/2$, $\delta N=(N_1-N_2)/2$, a and T and try to identify the region where there is a phase transition from the superfluid phase to the normal phase. This is interesting because of two reasons. First, since the polarization rises rapidly at this phase transition boundary, this boundary can be recognized in the trap by observing the polarization as a function of r. Second, the inhomogeneous phases are likely to be found near this boundary at low temperatures, and we would like to estimate the range of r where these phases are likely to exist. We choose $a=-0.5139$ eV^{-1}, for which the atomic system, especially near the center of the trap, cannot be considered weakly coupled, and hence our approximations may not be quantitatively accurate near the center of the trap. But the large coupling amplifies the features in the polarization profile that we are looking for. We use these features to deduce qualitative conclusions which may be more general than our approximations.

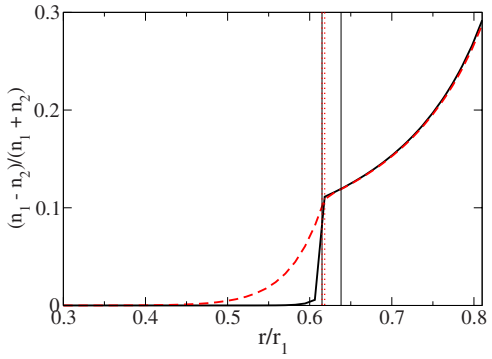

FIG. 8. (Color online) Polarization as a function of the r plotted in units of r_1. The bold line (black) corresponds to $T=0.1\delta\mu$ and the dashed line (red) to $T=0.36\delta\mu$. Also shown are regions where the system is unstable to the growth of inhomogeneities. The thin continuous lines (black) specify this region for $T=0.1\delta\mu$ and the thin dashed lines (red) mark this region for $T=0.36\delta\mu$. The lower boundary marked by a thin dotted line, coincides with the left-hand boundary of the thin continuous line. The upper boundary, however, appears at a larger r for the continuous line, telling us that the window of inhomogeneous pairing is wider at lower temperature. For $T=0.1\delta\mu$ the total value of $\bar{N}$ in the trap is 4.04×10^7 and the value of δN is 1.25×10^6. For $T=0.36\delta\mu$ the total value of $\bar{N}=4.03\times10^7$ and the value of $\delta N=1.53\times10^6$.

Although the true experimental variables are $\bar{N}$ and δN, we find it more convenient to fix the values of the average chemical potential at the center of the trap, μ_0, and the chemical potential splitting $\delta\mu$, and calculate $\bar{N}$ and δN in terms of these. The average chemical potential at a point r in the trap is $\mu(r)=\mu_0-V(r)$. Plotted in Fig. 8 is p as a function of r for $\mu_0=2.091\times10^{-10}$ eV and $\delta\mu=1.9\times10^{-11}$ eV for two different temperatures, $T=0.1\delta\mu$ and $T=0.36\delta\mu$. We focus on the region near the place where we observe the jump in the value of the polarization. The radius r has been plotted in units of r_1 defined as the radius where the effective chemical potential of ψ_1 species is zero, i.e., $r_1=r_0\sqrt{[2(\mu_0+\delta\mu)/\omega]}=33.253r_0$.

We see that, as expected, the jump in the polarization at the phase transition boundary becomes less sharp as we increase the temperature. We also mark the region where the system is unstable to the formation of inhomogeneous phases. We also see that the range of r where inhomogeneity may develop, decreases in size as we increase the temperature.

[1] J. Bardeen, L. N. Cooper, and J. R. Schrieffer, Phys. Rev. **108**, 1175 (1957).
[2] P. Fulde and R. A. Ferrell, Phys. Rev. **135**, A550 (1964).
[3] A. Larkin and Y. Ovchinnikov, Sov. Phys. JETP **20**, 762 (1965).
[4] H. Müther and A. Sedrakian, Phys. Rev. Lett. **88**, 252503 (2002).
[5] A. Sedrakian, J. Mur-Petit, A. Polls, and H. Müther, Phys. Rev. A **72**, 013613 (2005).
[6] J. Carlson and S. Reddy, Phys. Rev. Lett. **95**, 060401 (2005).
[7] D. T. Son and M. A. Stephanov, Phys. Rev. A **74**, 013614 (2006).
[8] G. B. Partridge, W. Li, R. I. Kamar, Y. Liao, and R. G. Hulet, Science **311**, 503 (2006).
[9] Y. Shin, M. W. Zwierlein, C. H. Schunck, A. Schirotzek, and W. Ketterle, Phys. Rev. Lett. **97**, 030401 (2006).
[10] G. B. Partridge, W. Li, Y. A. Liao, R. G. Hulet, M. Haque, and H. T. C. Stoof, Phys. Rev. Lett. **97**, 190407 (2006).
[11] Y. Shin, C. H. Schunck, A. Schirotzek, and W. Ketterle, Phys. Rev. Lett. **99**, 090403 (2007).
[12] Y.-I. Shin, C. H. Schunck, A. Schirotzek, and W. Ketterle, http://xxx.lanl.gov/abs/0709.3027
[13] R. Combescot and C. Mora, Eur. Phys. J. B **28**, 397 (2002).
[14] C. Mora and R. Combescot, Phys. Rev. B **71**, 214504 (2005).
[15] R. Combescot and C. Mora, Phys. Rev. B **71**, 144517 (2005).
[16] P. F. Bedaque, H. Caldas, and G. Rupak, Phys. Rev. Lett. **91**, 247002 (2003).
[17] J. Liao and P. Zhuang, Phys. Rev. D **68**, 114016 (2003).
[18] W. Yi and L.-M. Duan, Phys. Rev. A **73**, 031604 (2006).
[19] L. He, M. Jin, and P. Zhuang, Phys. Rev. B **74**, 214516 (2006).
[20] A. Sedrakian, H. Müther, and A. Polls, Phys. Rev. Lett. **97**, 140404 (2006).
[21] C.-C. Chien, Q. Chen, Y. He, and K. Levin, Phys. Rev. Lett. **97**, 090402 (2006).
[22] M. M. Parish, F. M. Marchetti, A. Lamacraft, and B. D. Simons, Nat. Phys. **3**, 124 (2007).
[23] K. B. Gubbels, M. W. J. Romans, and H. T. C. Stoof, Phys. Rev. Lett. **97**, 210402 (2006).
[24] G. Sarma, J. Phys. Chem. Solids **24**, 1029 (1963).
[25] H. Burkhardt and D. Rainer, Ann. Phys. **506**, 181 (1994).
[26] A. I. Buzdin and H. Kachkachi, Phys. Lett. A **225**, 341 (1997).
[27] R. Combescot and C. Mora, EPL **68**, 79 (2004).
[28] L. Gorkov and T. Melik-Barkhudarov, Sov. Phys. JETP **13**, 1018 (1961).
[29] H. Heiselberg, C. J. Pethick, H. Smith, and L. Viverit, Phys. Rev. Lett. **85**, 2418 (2000).
[30] A. Sedrakian, T. Alm, and U. Lombardo, Phys. Rev. C **55**, R582 (1997).
[31] A. Sedrakian and U. Lombardo, Phys. Rev. Lett. **84**, 602 (2000).
[32] R. Balian, H. Flocard, and M. Véneroni, Phys. Rep., **317**, 251 (1999).
[33] I. Shovkovy and M. Huang, Phys. Lett. B **564**, 205 (2003).
[34] M. Huang and I. Shovkovy, Nucl. Phys. A **729**, 835 (2003).
[35] K. Fukushima, C. Kouvaris, and K. Rajagopal, Phys. Rev. D **71**, 034002 (2005).
[36] D. Blaschke, S. Fredriksson, H. Grigorian, A. M. Öztas, and F. Sandin, Phys. Rev. D **72**, 065020 (2005);
[37] H. Abuki and T. Kunihiro, Nucl. Phys. A **768**, 118 (2006).
[38] S. B. Ruster, V. Werth, M. Buballa, I. A. Shovkovy, and D. H. Rischke, Phys. Rev. D **73**, 034025 (2006).
[39] H. J. Warringa, e-print arXiv:hep-ph/0606063.
[40] S. Reddy and G. Rupak, Phys. Rev. C **71**, 025201 (2005).
[41] E. Gubankova, M. Mannarelli, and R. Sharma, e-print arXiv:0804.0782.
[42] B. M. Fregoso and G. Baym, Phys. Rev. A **73**, 043616 (2006).
[43] H.-J. Schulze, A. Polls, and A. Ramos, Phys. Rev. C **63**, 044310 (2001).